NMR/MRI Study of Clathrate Hydrate Mechanisms

Shuqiang Gao,[†] Waylon House,*[,‡] and Walter G. Chapman*[,†]

Chemical Engineering Department, Rice University, Houston, Texas 77251, and Petroleum Engineering Department, Texas Tech University, Lubbock, Texas 79406

Received: April 21, 2005; In Final Form: August 12, 2005

Clathrate hydrates are of great importance in many aspects. However, hydrate formation and dissociation mechanisms, essential to all hydrate applications, are still not well understood due to the limitations of experimental techniques capable of providing dynamic and structural information on a molecular level. NMR has been shown to be a powerful tool to noninvasively measure molecular level dynamic information. In this work, we measured nuclear magnetic resonance (NMR) spin lattice relaxation times (T_1's) of tetrahydrofuran (THF) in liquid deuterium oxide (D_2O) during THF hydrate formation and dissociation. At the same time, we also used magnetic resonance imaging (MRI) to monitor hydrate formation and dissociation patterns. The results showed that solid hydrate significantly influences coexisting fluid structure. Molecular evidence of residual structure was identified. Hydrate formation and dissociation mechanisms were proposed based on the NMR/MRI observations.

Introduction

Gas hydrates are icelike structures in which water molecules, under pressure, form structures composed of polyhedral cages surrounding gas molecule "guests" such as methane and ethane. Rarely encountered in everyday life, they occur in staggering abundance under the sea floor and permafrost environments where (P, T) conditions ensure their stability. The natural gas trapped in these deposits represents a potential source of energy many times greater than all known natural gas reserves. Hydrates can form as well in undersea piping and above ground gas pipelines where they pose a major problem for gas/oil producers.

Detailed understanding of hydrate melting and formation mechanisms on a molecular level is important for successfully tackling all hydrate challenges with accuracy and confidence.[1] However, hydrate growth and dissociation mechanisms still remain unclear because very few experimental techniques can provide in situ dynamic information on a molecular scale. Liquid water structure coexisting with the hydrate phase, especially near the water/hydrate interface, is very important in understanding the hydrate formation and dissociation processes. The imminent state before guest molecules solidify into the hydrate phase and the fluid structure immediately after clathrate hydrate dissolves into the liquid state may hold the key to unlock the secrets of hydrate mechanisms.

NMR has been shown to be a powerful tool to noninvasively measure molecular level dynamic information. T_1 is an indicator of local molecular order around the spin-bearing molecules.[2] T_1 measurement is an effective method to monitor microscopic fluid structure change. In this work, NMR T_1 measurements of THF in D_2O solution were employed to probe the change of water structure around THF during THF hydrate formation and dissociation to understand the role of the water and hydrate interface. Proton MRI[3] was also utilized to observe the hydrate formation and dissociation patterns.

* Corresponding authors. E-mail: Waylon.House@ttu.edu; wgchap@rice.edu.

[†] Rice University.

[‡] Texas Tech University.

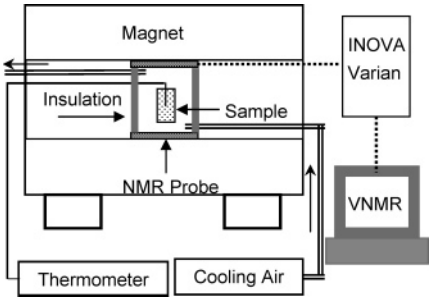

Figure 1. Experimental schematic.

THF molecules become invisible to liquid-state NMR as they are incorporated into the solid hydrate phase; thus, the T_1's of THF in the liquid phase can be measured independently of the THF hydrate. D_2O is invisible to proton NMR under all conditions, so only THF in the liquid phase is visible to MRI. Results showed that the presence of solid hydrate significantly influences the fluid structure. T_1 measurements also indicated the existence of residual effects after hydrate dissociation.

Experimental Details

The schematic of the experimental setup is shown in Figure 1. T_1 measurements of THF (Aldrich, 99+%) in D_2O (Cambridge Isotope Laboratories, D 99.9%) and MRI imaging experiments were performed on an 85 MHz Oxford horizontal 31 cm wide bore NMR with imaging capability, using a LITZ RF volume coil (with 14 cm internal diameter) from Doty Scientific, Inc. Data were acquired and processed using Varian VNMR software and INOVA hardware systems. T_1's were measured using the inversion and recovery technique. VNMR software, given inputs of possible minimum and maximum T_1 values, automatically generates standard $180°-\tau-90°$ pulse sequences with various values of delay time τ. It took 4 to ~6 min to take a T_1 data point and about 1 h to take an MRI image.

An air-jet temperature controller supplied dry and cold air to control the sample temperature. It is capable of controlling temperature from −40 to 100 °C with 0.1 °C stability. A glass

10.1021/jp052071w CCC: $30.25
Published on Web 09/28/2005

bottle with a cap that has a Teflon liner was used to contain 29 mL of THF−D_2O solution (molar ratio 1:17) and was tightly sealed to prevent THF evaporating into the environment. The sample was weighed, and no THF loss was detected after a long period of time. A LUXTRON fluoroptic thermometer was mounted into the glass container through the cap to monitor the sample temperature. Its output reading resolution is 0.1 °C.

Since trace amounts of oxygen may alter the T_1 of THF significantly, pure D_2O and THF liquids were deoxygenated separately in a closed glovebox with a nitrogen environment. D_2O and THF were contained in two separate Teflon bottles. The gas phase above the liquid phase was periodically flushed with nitrogen gas, and the bottles were periodically shaken to facilitate the diffusion of oxygen out of the liquid phase. After the gas phase had been flushed 6 or 7 times over about 12 h, THF and D_2O were mixed on the molar basis of 1:17 in the glass bottle. This is the same concentration of THF in D_2O in the hydrate phase. Therefore, as hydrate forms the liquid-phase composition will not change. The sample was then sealed and moved into the probe for T_1 measurements. (The success of deoxygenation was demonstrated by that fact that after deoxygenation, the T_1 of THF in liquid D_2O increased about 2 s compared to that of the sample without deoxygenation.)

In a recent paper,[4] we reported that the T_1 of THF in D_2O after THF hydrate dissociation is consistently smaller than that before hydrate formation. It was suggested that the change in T_1 is due to the THF−D_2O solution becoming more microscopically homogeneous after hydrate dissociation than before hydrate formation. To investigate residual clathrate hydrate structure after hydrate dissociation by T_1 measurements, it is important to ensure that the THF−D_2O solution is already homogeneous and in its equilibrium configuration before hydrate formation. Then, if the T_1 after hydrate dissociation is different from that before hydrate formation, it would be strong evidence of residual clathrate hydrate structure. Therefore, in this study, the freshly mixed THF−D_2O solution was first turned into hydrate and subsequently dissociated, to make the sample solution microscopically homogeneous before T_1 and MRI measurements. To eliminate any possible residual clathrate structure, the THF−D_2O solution was heated to 35 °C after hydrate dissociation and equilibrated at room temperature for 24 h. T_1 measurement was then started as the sample was cooled in steps until hydrate nucleation, which was indicated by a sudden rise of the sample temperature. The temperature of the cooling air was then adjusted to slow the hydrate formation rate for better T_1 measurement and imaging experiments. After complete hydrate formation, marked by the disappearance of THF peaks in the NMR spectrum, the temperature was raised to slowly dissociate the hydrate. Right after complete hydrate dissociation, the temperature was cooled to form hydrate again, to examine the memory effect. After the reformation was complete, THF was dissociated and the temperature was raised to room temperature in steps. Images of hydrate formation and dissociation patterns were taken by the MRI technique using the spin−echo multislice (SEMS) pulse sequence. The parameters were adjusted to produce proton density-weighted images, which depend primarily on the density of protons in the imaging volume with the effects of T_1 and T_2 minimized. The orientation of the image slice was in the horizontal direction.

Results and Discussion

The dependence of $\ln(1/T_1)$ on $1/T$ (T is temperature in K) during cooling, hydrate formation, hydrate dissociation, and warming up, is plotted in Figure 2. The relationship is linear

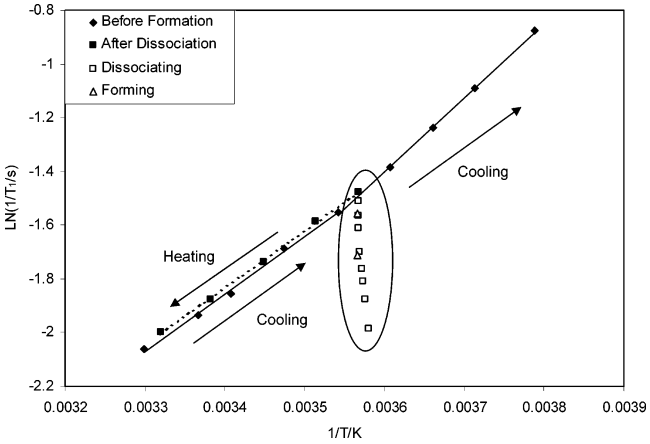

Figure 2. T_1 behavior of THF at various temperatures and conditions.

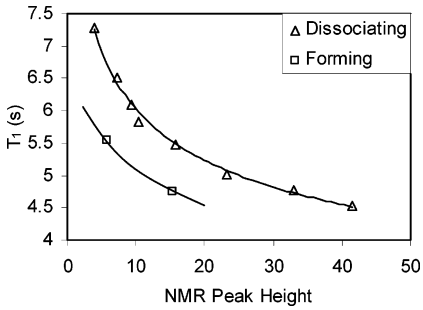

Figure 3. T_1 as a function of NMR peak height, i.e., the amount of liquid, during hydrate formation and dissociation.

during cooling and warming up. Every T_1 data point was measured with a standard deviation less than 0.05 s. It required substantial subcooling to initiate hydrate formation. The reported slope change around 8−9 °C during cooling was reproduced.[4] The free induction decay and sign of the slope indicate the motion of THF in D_2O solution is in the extreme narrowing region, i.e., the rotational correlation time of THF, τ_c, is less than 10^{-9} s. On the basis of NMR theory,[5] the rotational activation energy of THF, E_a, can be calculated from the slope if the relation $\tau_c = \tau_o \exp(E_a/RT)$ is assumed, where R is the universal gas constant. The resulting E_a's for the cooling and warming up processes in the temperature range of 8−25 °C are about the same, 17.76 and 17.74 kJ/mol, respectively. There still is a slight shift in T_1 after hydrate dissociation compared to that before hydrate formation. However, the difference is minuscule compared to the T_1 change after dissociating the hydrate that formed from fresh THF−D_2O solution.[4] It is probably because in this experiment THF was already homogeneously distributed before hydrate formation, and its distribution did not change much after hydrate dissociation.

One interesting feature in Figure 2 is that the T_1 values of THF in the liquid phase during hydrate formation and dissociation fall far off the linear lines for the cooling and heating processes in the single liquid phase. Since the concentration of THF in the liquid phase remains unchanged during hydrate formation/dissociation, this reveals that the presence of solid hydrate strongly influences its coexisting fluid structure. The liquid/hydrate interface probably played an important role through the O−H bonds of the partial cages on the hydrate surface sticking into and structuring the liquid phase. Figure 3 shows the change of T_1 as a function of peak height, i.e., the amount of remaining liquid, during hydrate formation and dissociation. As the amount of liquid diminishes and more hydrate is present, the T_1 of THF gets higher. One possibility

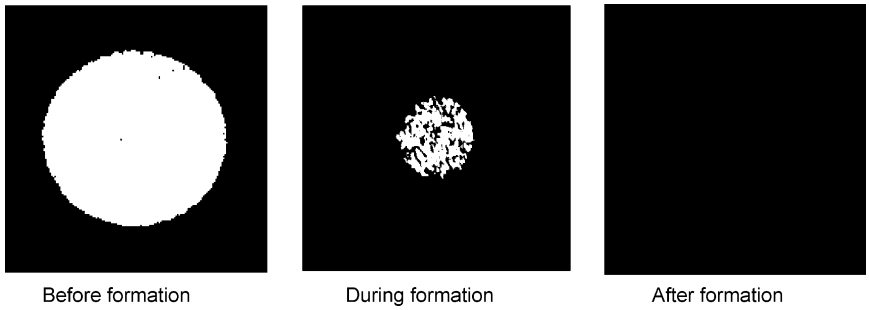

Figure 4. THF hydrate formation pattern from THF−D_2O solution. The white area is the liquid phase. THF hydrate is invisible to MRI.

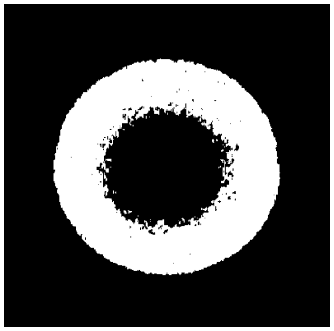

Figure 5. Hydrate dissociation pattern as the sample is warmed from the perimeter.

is a higher percentage of the water being structured by the hydrate surface, as more hydrate is present. This structured interface hypothesis is in agreement with the "reaction film" proposition by Clarke and Bishnoi[6] for hydrate growth. Figure 3 also reveals that T_1's during hydrate dissociation are higher than those during hydrate formation under the same conditions and phase composition. This difference in T_1 between formation and dissociation transitions indicates a difference in fluid structure. This difference can be argued as the evidence of residual hydrate structure. However, this residual structure does not necessarily mean clathrate aggregates remaining in solution.[7] It could be residual hydrogen bonds from collapsing of the solid clathrate structures. After complete hydrate dissociation, T_1 returned to normal values within 16 h without further raising the temperature.

MRI images of hydrate formation and dissociation patterns were also taken for better understanding of hydrate growth and dissociation mechanisms. A higher degree of subcooling and a longer induction time were required to form THF hydrate for the first time. Once hydrate started to form, formation was rapid because the sample temperature was lower than the equilibrium temperature. MRI images of hydrate formation are shown in Figure 4. It was demonstrated that hydrate nucleated homogeneously along the perimeter of the sample and formed from the outside inward.

After hydrate formation was complete, the temperature was raised to melt the hydrate. As shown in Figure 5, hydrate started to melt along the perimeter. The dissociation progressed along the hydrate/liquid interface toward complete dissociation, which was indicated by the NMR peak heights returning to the original values before hydrate formation. To examine the memory effect and hydrate reformation pattern, the sample was cooled to form hydrate again right after the dissociation was complete. This time it required shorter induction time and less subcooling. The hydrate formation was also gradual compared to last time. The formation kinetics could be well controlled by changing the cooling air temperature. The MRI images of hydrate reformation are displayed in Figure 6. The nucleation took place at a point near the wall of the sample bottle instead of homogeneously along the sample perimeter as it formed hydrate for the first time. This may be due to a hydrate residual structure mentioned earlier, which functioned as a nucleation seed. Both T_1 and MRI experiments were repeated several times to confirm their reproducibility.

In summary, T_1 measurements of THF in the liquid phase during hydrate formation and dissociation strongly suggest that the presence of solid hydrate coexisting with the liquid phase influences the fluid structure, probably through hydrogen bonding between the liquid and the solid at the interface, which creates a structured liquid layer. As expected, MRI images showed that once hydrate nucleates, hydrate grows only at the hydrate/water interface, even though the THF concentration is homogeneous in the liquid phase. Hydrate only dissociates at the interface even though the temperature is uniform in the solid hydrate. Tohidi et al.[8] discovered that hydrates isolated from the liquid phase require higher than equilibrium temperature to dissociate, which demonstrated the important role of the liquid/hydrate interface for hydrate dissociation. Ikeda-Fukazawa and Kawamura[9] simulated ice melting using molecular dynamics. It was concluded that the dangling motion of the free O−H

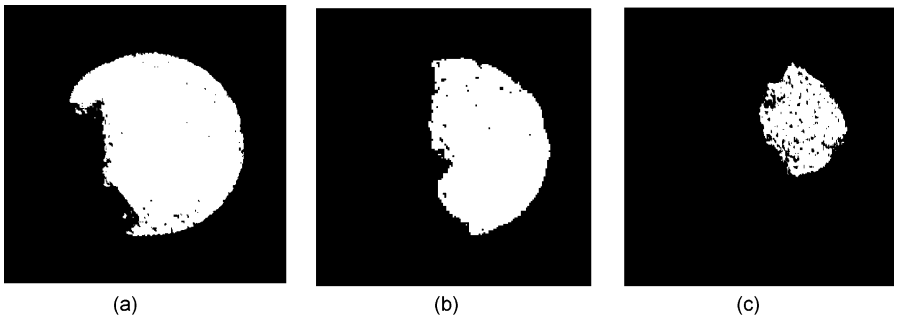

Figure 6. Reformation pattern of THF hydrate from the THF−D_2O solution that formed hydrate before. Hydrate formation progresses from (a) to (c).

bonds on the ice surface is the main cause of destructing ice crystal structure.

The above observations lead to the following hypothesis about the hydrate mechanism. The structured liquid water at the hydrate surface is the key to hydrate growth and dissociation. During hydrate growth, water and THF molecules near the hydrate surface are structured into a semiclathrate organization while the water network away from the interface is still in the normal liquid state. This structured liquid layer causes hydrate to preferentially form at the interface instead of elsewhere, and it facilitates hydrate growth. During hydrate dissociation, kinetic energy is transmitted through the motions of the hydrogen bonds in the structured layer to break down the solid clathrate structure.

Conclusions

T_1 measurements and MRI techniques were employed to investigate THF hydrate formation and dissociation to improve the understanding of clathrate hydrate mechanisms. It was found that the simultaneous presence of water and hydrate significantly increases the T_1 of THF in the coexisting liquid phase—the more hydrate, the higher the T_1. This is probably because the lower the liquid fraction, the greater the structuring of the liquid phase, which causes T_1 to increase further. MRI images demonstrated that hydrate grows and dissociates along the hydrate/water interface. Combined with results from T_1 measurements, it was proposed that the structured water layer in contact with the hydrate surface is the key to both hydrate growth and dissociation. The structured layer causes hydrate to preferentially form at the hydrate/water interface and facilitates hydrate growth. During hydrate dissociation, the kinetic energy of liquid water is transferred through the structured layer to collapse the hydrogen-bonding network in the solid hydrate.

Reformation of THF hydrate right after hydrate dissociation required less subcooling and shorter induction time than the initial hydrate formation. This memory effect is probably due to the existence of residual structures in the hydrate melt, which is supported by the higher T_1 of THF during hydrate dissociation than during hydrate formation.

Acknowledgment. We thank the Robert A. Welch Foundation (Grant C-1241) and the Livermore Chair (TTU) for financial support.

References and Notes

(1) Koh, C. A. Towards a fundamental understanding of natural gas hydrates. *Chem. Soc. Rev.* **2002**, *31*, 157.

(2) Hertz, H. G. Microdynamic behavior of liquids as studied by NMR relaxation times. *Prog. Nucl. Magn. Reson. Spectrosc.* **1967**, *3*, 159.

(3) Moudrakovski, I. L.; Ratcliffe, C. I.; McLaurin, G. E.; Simard, B.; Ripmeester, J. A. Hydrate layers on ice particles and superheated ice: a ^{1}H NMR microimaging study. *J. Phy. Chem. A* **1999**, *103*, 4969.

(4) Gao, S.; House, W.; Chapman, W. G. NMR and viscosity investigation of clathrate hydrate formation and dissociation. *Ind. Eng. Chem. Res.* **2005**, *44*, 7373.

(5) Fukushima, E.; Roeder, S. B. W. *Experimental Pulse NMR—A Nuts and Bolts Approach*; Westview Press: Boulder, Colorado, 1981.

(6) Clarke, M. A.; Bishnoi, P. R. Determination of the intrinsic kinetics of CO_2 gas hydrate formation using in situ particle size analysis. *Chem. Eng. Sci.* **2005**, *60*, 695.

(7) Makogon, Y. F. *Hydrates of Natural Gas*; PennWell Books: Tulsa, Oklahoma, 1981.

(8) Tohidi, B.; Burgass, R. W.; Danesh, A.; Ostergaard, K. K.; Todd, A. C. Improving the accuracy of gas hydrate dissociation point measurements. *Ann. N.Y. Acad. Sci.* **2000**, *912*, 924.

(9) Ikeda-Fukazawa, T.; Kawamura, K. Molecular-dynamics studies of surface of ice Ih. *J. Chem. Phys.* **2004**, *120*, 1395.